"FUEL ROD MECHANICAL DEFORMATION DURING THE PBF/LOFT LEAD ROD LOSS-OF-COOLANT EXPERIMENTS"

CONF-800723--18

D. J. Varacalle, Jr., P. E. MacDonald, S. Shiozawa, W. E. Driskell
EG&G Idaho, Inc.
P.O. Box 1625
Idaho Falls, Idaho 83401

ABSTRACT

Results of four PBF/LOFT Lead Rod (LLR) sequential blowdown tests conducted in the Power Burst Facility (PBF) are presented. Each test employed four separately shrouded fuel rods. The primary objective of the test series was to evaluate the extent of mechanical deformation that would be expected to occur to low pressure (0.1 MPa), light water reactor design fuel rods when subjected to a series of double ended cold leg break loss-of-coolant accident (LOCA) tests, and to determine whether subjecting these deformed fuel rods to subsequent testing would result in rod failure. The extent of mechanical deformation (buckling, collapse, or waisting of the cladding) was evaluated by comparison of cladding temperature and system pressure measurements with out-of-pile experimental data, and by posttest visual examinations and cladding diametral measurements. The tests were performed at system conditions of 595 K coolant inlet temperature, 15.5 MPa system pressure, and 41 to 57 kW m test rod peak linear power, at initiation of blowdown. Maximum measured cladding temperatures during the tests ranged from 870 to 1260 K. None of the rods failed during the tests. Posttest examination indicated that the rods were uniformly covered with a black oxide and five of the seven test rods used for the test series experienced cladding collapse. The PBF/LOFT Lead Rod Test Series demonstrated that low pressure, light water reactor design fuel rods can withstand multiple blowdown transients at power densit as high as 57 kW/m without failure.

DISCLAIMER

INTRODUCTION

The behavior of light water reactors (LWRs) following a postulated loss-of-coolant accident (LOCA) must conform to criteria specified in the Code of Federal Regulations. To ensure that the behavior of both the cooling system and the nuclear core is understood and properly modeled, in-pile experiments are being conducted in the Loss-of-Fluid Test (LOFT) Facility and Power Burst Facility (PBF) at the Idaho National Engineering Laboratory by EG&G Idaho, Inc., for the U.S. Nuclear Regulatory Commission (NRC). The LOFT Facility was designed to represent the behavior of an entire large pressurized water reactor (PWR) during a postulated LOCA. The PBF-LOCA tests are providing in-pile information on the thermal and mechanical deformation behavior of nuclear fuel rods subjected to coolant conditions representative of the conditions expected in a LWR during a double ended cold leg break LOCA.

The extent of the mechanical deformation and the propensity for failure of the LOFT fuel during the planned series of nuclear blowdown tests has been of concern. Therefore, a series of special tests, designated the LOFT Lead Rod (PBF/LLR) tests, were first conducted in the Power Burst Facility to provide information on the behavior of low internal pressure, LWR type fuel rods subjected to multiple blowdowns and power ramps. The test program provided an indication of the consequences of continued operation of a nuclear core with deformed fuel rods. The tests were conducted for the U.S. Nuclear Regulatory Commission with funding provided by the Japanese Atomic Energy Research Institute.

The primary objectives for the PBF/LLR tests were: (a) to experimentally evaluate the extent of cladding collapse that would be expected to occur during the LOFT LOCA transients, (b) to evaluate the effects of collapsed cladding and pellet-cladding interaction (PCI) on the mechanical response of deformed fuel rods during subsequent power increases, long term preconditioning, and loss-of-coolant conditions, (c) to provide experimental data to benchmark codes that will be used for requalification of the LOFT core, and (d) to evaluate the behavior and reliability of the LOFT fuel rod thermocouples.

The purpose of this paper is to show that previously deformed low internal pressure fuel rods will not fail when subjected to successive LOCEs, and to quantify the amount of deformation expected to occur during a full power (52 kW/m) double ended cold leg break LOCA.

Tests LLR-3, LLR-5, LLR-4 and LLR-4A were performed at system conditions of 595 K coolant inlet temperature, 15.5 MPa system pressure and 41, 46, 57 and 56 kW/m test rod peak linear power, respectively at initiation of blowdown. Each test employed four separately shrouded, unpressurized LWR type fuel rods. The rods were exposed to thermal-hydraulic boundary conditions representative of a severe, instantaneous double ended cold leg break in a PWR.

The elevated cladding temperatures witnessed during the LLR tests coupled with the corresponding system depressurization as a function of time, resulted in significant fuel rod mechanical deformation. This mechanical deformation was minor during the low power tests, but continued to accumulate throughout the high power tests, with the maximum deformation attained in the LLR-4A test.

Maximum measured cladding temperatures for Test LLR-3 ranged from 870 to 990 K. On the basis of these cladding temperatures, fuel rod mechanical deformation probably did not occur during this test. Maximum cladding temperatures in the range of 985 to 1015 K were measured during Test LLR-5, which probably resulted in two-point buckling of the cladding at the thermocouple locations. However, the cladding elongation measurements during this test and the subsequent tests of the LLR series indicated that DNB occurred earlier and at lower elevations than indicated by the thermocouple measurements. Higher cladding temperatures and cladding collapse were thus probable at locations lower than the thermocouples during test LLR-5. Maximum measured cladding temperatures ranged from 1065 to 1165 K during Test LLR-4. One rod (312-1) was removed after the test for postirradiation examination. The rod was waisted from 35 to 55 cm. Comparable deformation is expected to have occurred to the other three rods during this test. Maximum measured cladding temperatures for Test LLR-4A ranged from 1070 to 1260 K. Subsequent examination of the four rods of this test during the postirradiation

examination revealed that all four rods had achieved either the collapse or waisting regime of mechanical deformation but none of the rods failed.

A brief description of the test hardware and conduct is presented in the next section. The thermal hydraulic response of the coolant during the LLR-5 test is presented in the following section; it is considered typical of the thermal hydraulic behavior in all the LLR tests. Included are discussions of the coolant depressurization, temperature, and volumetric flow in the flow shrouds. The behavior of the fuel rods is then described and includes discussions of steady state behavior as a function of rod power which provides an indication of cladding deformation from test to test, and transient thermal and mechanical response. Comparisons with FRAP and RELAP4 are also included.

TEST DESCRIPTION

Each test was performed with four identical, unpressurized, PWR-type fuel rods pressurized to 0.103 MPa, each surrounded by an individual circular flow shroud. The test rods were symmetrically positioned at the center of the PBF reactor in an environment with typical PWR coolant pressures, temperatures, and flow rates. The LLR test rods consisted of a 0.914 m long stack of 93% theoretical density uranium dioxide fuel pellets enriched with 9.5 wt% U^{235} and clad with Zircaloy-4. The rods were unirradiated at the start of the tests.

The experimental hardware is composed of the PBF in-pile tube and its contents, the primary coolant system, the blowdown system, and the reflood and quench system. The inlet (cold) and outlet (hot) coolant pipes attached to the in-pile tube are connected directly to the blowdown system and the primary coolant system. During the course of the test, the various systems are connected or disconnected to the in-pile tube by means of high speed valves. Figure 1 illustrates the PBF in-pile tube and blowdown system. Figure 2 illustrates the test train assembly for the LLR tests. Figure 3 presents an illustration of a test fuel rod within a circular shroud, and the associated instrumentation.

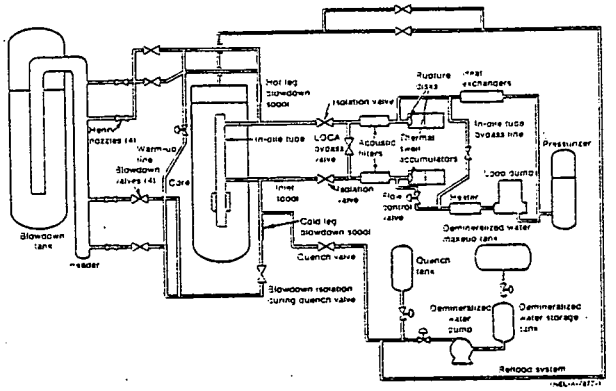

Figure 1. PBF-LOCA blowdown loop.

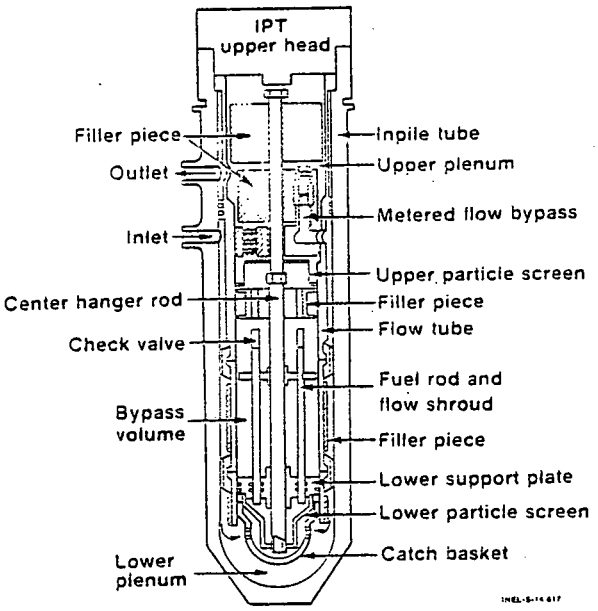

Figure 2. Test train assembly for LLR tests.

Each of the four PBF/LLR tests involved a preconditioning phase to promote pellet cracking and relocation and steady state operation to build up a fission product inventory. The preconditioning phase consisted of several power cycles to provide fuel preconditioning and intercalibration of the test rods with the PBF core power. The rods were then irradiated for a few hours at a test rod peak power density of 41 kW/m during Test LLR-3, 47 kW/m during Test LLR-5, 57 kW/m during Test LLR-4, and 56 kW/m during Test LLR-4A. For each test, system conditions typical of a PWR prior to blowdown were approximately: 595 K inlet coolant temperature, coolant flowrate through each flow shroud of 0.584 l/s for Tests LLR-3 and LLR-5, and 0.78 l/s for Tests LLR-4 and LLR-4A, and system pressure of 15.5 MPa.

Transient test operation was initiated with isolation of the in-pile tube and experimental hardware from the PBF primary coolant system, and a simultaneous system blowdown. Blowdown commenced with the opening of the two high speed (~100 ms) blowdown valves, shown in Figure 1, in the cold leg of the coolant loop, to simulate a 200% double-ended cold leg break LOCA. Approximately 3.75 seconds after initiation of blowdown, the large cold leg blowdown valve was closed until 22 seconds, when it was reopened. This valve sequencing was necessary to match the LOFT required system depressurization. The throats of converging-diverging nozzles located downstream from the valves were sized to control the blowdown flow and depressurization rates. The coolant ejected from the in-pile tube was collected in the system blowdown tank. Reflood was performed by injecting coolant from a quench tank directly into the in-pile tube. After reflood, additional posttest quench cooling was provided to completely flood the fuel rods and terminate the test.

THERMAL-HYDRAULIC RESPONSE DURING THE LLR TESTS

The PBF/LLR program focused on fuel rod behavior rather than system behavior. The performance of LOCA experiments in the PBF differs from blowdown experiments witnessed in the LOFT program in that only the reactor core portion of the experiment is depressurized in PBF, whereas the entire system is blown down in the LOFT facility, as would occur during a LOCA in a

commercial PWR. The variables that affect fuel rod behavior include coolant pressure, density, temperature, and flow. The coolant pressure, in conjunction with the fuel rod internal pressure and cladding temperature, provides the driving force that governs the fuel rod cladding deformation. The coolant thermal-hydraulic behavior during the four PBF/LLR tests was similar. For this reason, only selected results from Test LLR-5 are presented. To better understand the test results and to evaluate code capabilities, analytical calculations were made with the RELAP4 MOD6[2,a] and FRAP-T5[3,b] computer codes. The RELAP4 code was used for calculations of coolant thermal-hydraulic response and associated fuel rod thermal behavior. The FRAP code was used to predict the coupled thermal-mechanical behavior of the LLR test rods.

Figure 4 presents the measured and calculated (RELAP4) system depressurization in the lower plenum during Test LLR-5. The steady state pressure prior to blowdown was approximately 15.5 MPa. With the initiation of the cold leg blowdown transient, the system depressurized to the vapor pressure of the coolant (12.5 MPa corresponding to a saturation temperature of 601 K) in approximately 50 ms. The cold leg flow became choked at the converging - diverging nozzles at approximately 50 ms. The system was fully depressurized by about 30 s.

The fuel rod shroud flows during the blowdown were primarily controlled by the depressurization of the lower plenum. Upon initiation of blowdown, the coolant in the flow shrouds reversed direction, check valves located on the top of each shroud closed, and the shroud flow was isolated from the upper plenum throughout the blowdown transient. The shroud outlet volumetric flow rate for Rod 312-1 during Test LLR-5 is shown in Figure 5 with the corresponding RELAP4 prediction. Upon initiation of blowdown, flashing first occurred in the fuel rod flow shroud where the highest enthalpy fluid was

---

a. RELAP4/MOD6, Update 4, Version III, Idaho National Engineering Laboratory Configuration Control Number H00441IB.
b. FRAP-T5, Idaho National Engineering Laboratory Configuration Control Number H0005838.

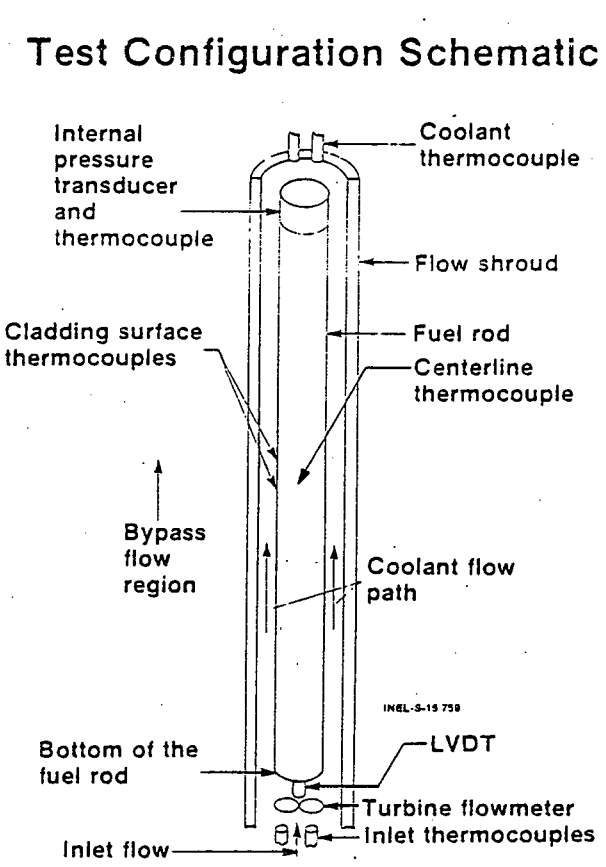

Figure 3. PBF/LLR test configuration schematic.

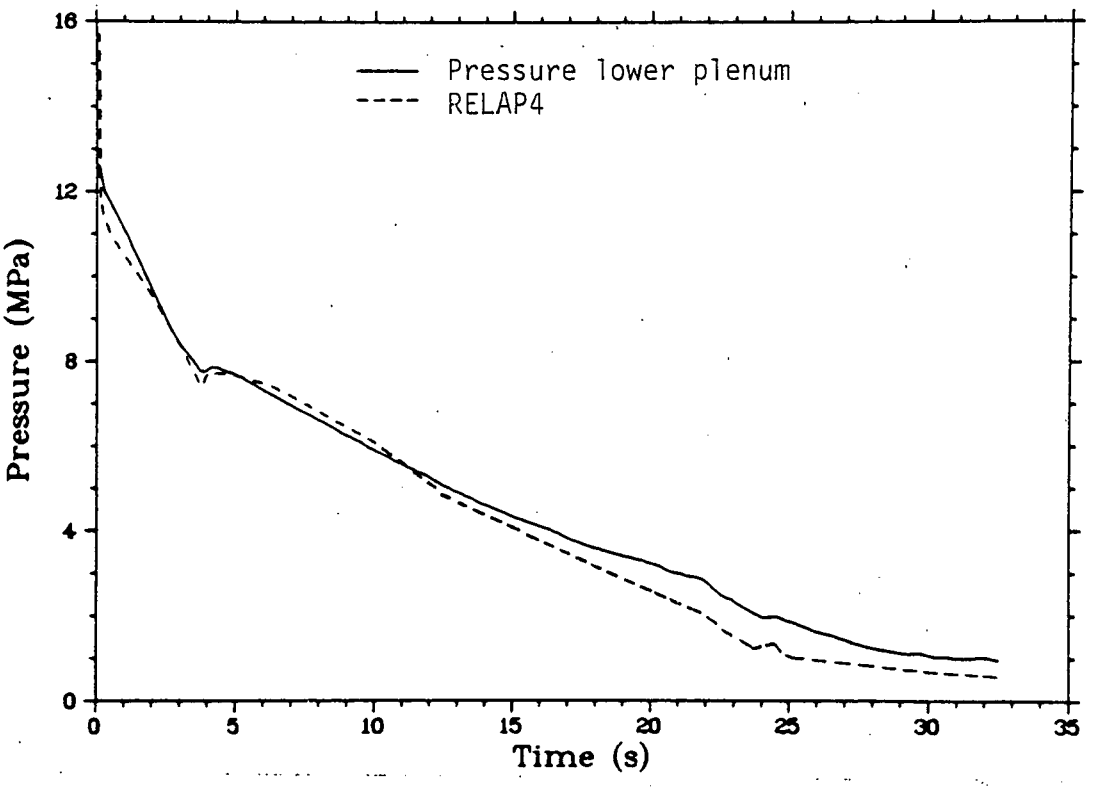

Figure 4. Comparison of lower plenum pressure for Test LLR-5 with RELAP4.

located and the lower turbine meter was immediately saturated at -1.5 l/s, its mechanical limit. The flow in the lower turbine then decreased to -0.8 l/s when the cold leg flow choked at the blowdown nozzles. Beyond this point the data indicate a substantial amount of volumetric flow until the large cold leg blowdown valve was closed at 3.75 s. The flow then decreased sharply and gradually stagnated for the remainder of the transient until 22 seconds, when the reopening of the blowdown valve generated volumetric flows comparable to those during the first 5 seconds.

As blowdown was initiated, the coolant temperatures within the flow shrouds reached saturation within 50 ms. Local qualities continued to rise during the first several seconds of the transient until they reached unity between 6.5 and 7 seconds. The coolant temperatures then increased significantly above the saturation temperature throughout the remainder of the transient. This superheating was attributed to energy transfer by convection and radiation from the fuel rods and flow shrouds. Figure 6 presents an indication of the radial temperature distribution from the fuel rod to the volumetric bypass during the LLR-5 test for flow shroud 345-1. Radiation heat transfer from the hot fuel rods to the flow shrouds was significant once superheated conditions were attained in this shroud at 6.5 s. The RELAP4 pretest prediction for the 0.533 m location coolant temperature shown in Figure 6 indicated a quality of 1.0 would be reached at 5 s into the transient. Past this time, the analytical predictions indicated slightly increasing superheated steam temperatures due to the almost adiabatic condition in the shrouds.

FUEL ROD BEHAVIOR

During a loss-of-coolant situation, the cladding temperature history in combination with the pressure differential across the cladding controls the type and degree of fuel rod deformation.

The exposure of the LOFT fuel rods to high cladding temperatures and compressive stresses may cause uniform cladding collapse and waisting onto the

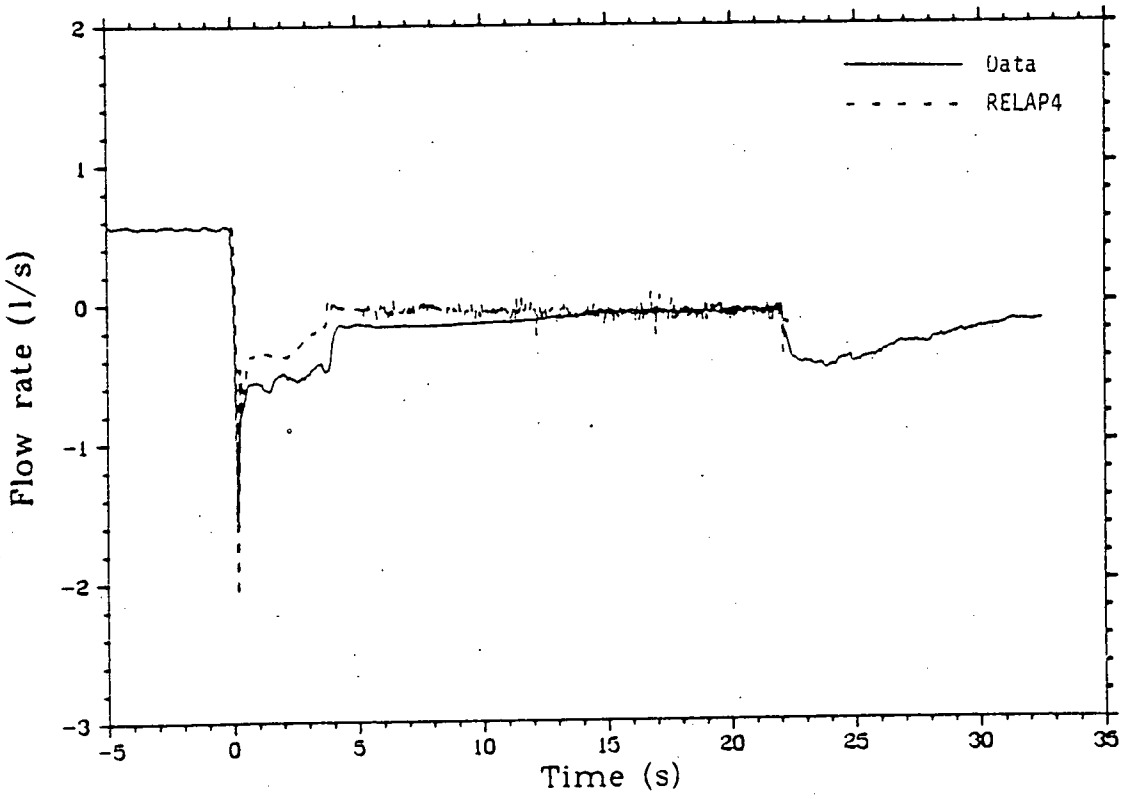

Figure 5. Comparison of calculated and measured lower turbine volumetric flow for Rod 312-1 during Test LLR-5.

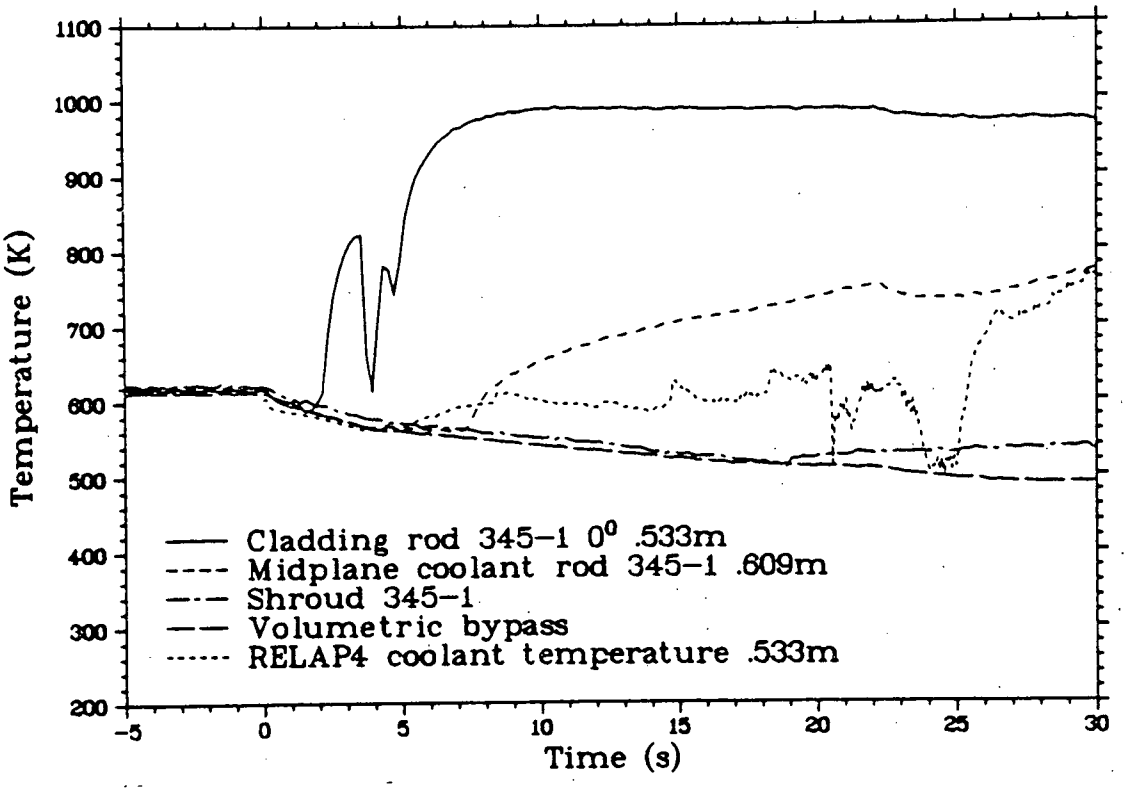

Figure 6. Coolant temperatures in shroud 345-1 for Test LLR-5.

fuel with a decrease in the cladding diameter. The PIE and fuel centerline temperature response during the steady state portion of the tests of the PBF LLR test rods provided information on when and under what conditions this deformation occurred. The deformation has been correlated with changes in cladding microstructure (i.e. temperature) from the PIE and the on-line temperature and elongation measurements, making possible a close estimate of the chronology of the cladding deformation process.

In subsequent sections, fuel rod thermal-mechanical responses observed during each test are discussed for selected fuel rods. The fuel rod deformation witnessed in the LLR transients is then discussed and compared with out-of-pile deformation data by Olsen,[4] postirradiation examination measurements, and steady-state fuel centerline temperatures.

Fuel Rod Thermal-Mechanical Response

Coolant, cladding surface and fuel centerline temperatures, and cladding length changes (an indication of time to CHF) were measured during the LLR tests. Representative measurements from two of the LLR test rods, Rod 312-1 which was subjected to the first three transients (LLR-3, LLR-5 and LLR-4) and Rod 345-1 which was subjected to the last three transients are presented in the following paragraphs. The cladding temperatures followed the coolant saturation temperature until DNB occurred. After DNB, cladding temperatures rose rapidly, reaching peak values at about 8 to 20 s. After peaking, the cladding temperatures decreased slowly until rod quench. In general, the peak cladding temperatures increased when the initial rod power was increased and were higher at lower axial elevations. A maximum temperature of 1260 K was measured at the 0.314-m location during the LLR-4A test. Table 1 lists the maximum measured cladding temperatures for the fuel rods utilized for the LLR tests.

RELAP4 comparisons of cladding temperature are provided for comparison with the data in the subsequent figures. In general, the time to CHF for the RELAP4 pretest predictions was in the vicinity of 0.5 s. This underpredicted the measured times to CHF which resulted in substantially higher predicted cladding temperatures than the data. For RELAP4 posttest analysis, CHF was

forced to occur at the times witnessed in the tests in an attempt to more closely match the data. In spite of this, cladding temperatures were again substantially higher than the data.

Figure 7 illustrates the cladding temperature, cladding elongation, and coolant midplane temperature response of Rod 312-1 during the first 30 seconds of the Test LLR-3 blowdown. The peak Rod 312-1 power was 40.3 kW/m just prior to blowdown. The cladding temperature data indicate that the rod achieved DNB at approximately 2.4 s at the 0°-0.533 m thermocouple location, and a maximum cladding surface temperature of 950 K, while the 180°-0.533 thermocouple indicated DNB at 2.8 s and a maximum surface temperature of 930 K. The cladding elongation transducer recorded a sharp increase at 2.8 s, which suggests that DNB occurred over a significant length of the fuel rod surface

TABLE 1. LLR FUEL ROD MAXIMUM MEASURED CLADDING TEMPERATURES

	Temperature (K)			
Rod	Test LLR-3	Test LLR-5	Test LLR-4	Test LLR-4A
Rod Power (kW/m)	41	47	57	56
312-1[a]	950	1000	1125	--
312-2[b]	920	1015	1165	1150
312-3[a]	990	--	--	--
312-4[a]	880	--	--	--
345-1[a]	--	1000	1060	1070
345-2[c]	--	(c)	(c)	(c)
399-2[d]	--	--	--	1260

a. Measured 0.533 m from bottom of heated length.
b. Measured 0.457 m from bottom of heated length.
c. Not instrumented with cladding thermocouples.
d. Measured 0.314 m from bottom of heated length.

at that time. This also indicates that the surface thermocouples did not affect the transient response of the rods during the LLR-3 test. If CHF had occurred earlier at a higher power location, an increase in cladding length would have been indicated prior to the indicated cladding temperature increase.

Figure 8 illustrates the cladding temperature and elongation response of Rod 312-1 during the first 30 seconds of Test LLR-5. The peak rod power for Rod 312-1 was calculated to be 47.3 kW/m just prior to blowdown. The cladding surface thermocouple data at the 0°-0.533 m thermocouple location indicated that the rod achieved DNB at 1.8 seconds and reached a maximum surface temperature of 1000 K at 10 seconds. The 180°-0.533 m thermocouple achieved DNB at 1.95 s and reached a maximum surface temperature of 990 K at 10 seconds. The LVDT first recorded a moderate increase in cladding length at 0.5 seconds, and then a stronger indication at 1.5 seconds. The rod departed from nucleate boiling at an elevation lower than the cladding thermocouples and the film boiling propagated up the rod. This indicates that the surface thermocouples delayed DNB in the upper portion of the rod and may have affected the transient response of the fuel rods.

Figure 9 illustrates the cladding temperature and elongation response of Rod 312-1 during the first 30 seconds of Test LLR-4. The peak rod power for Rod 312-1 was calculated to be 56.6 kW/m just prior to blowdown. The cladding surface thermocouple data at the 0°-0.533 m thermocouple location indicated that the rod achieved DNB at 1.65 seconds and reached a maximum surface temperature of 1125 K at 7 seconds. The 180°-0.533 m thermocouple achieved DNB at 1.65 s and reached a maximum surface temperature of 1120 K at 10 s. The LVDT first recorded a moderate increase in cladding length at 0.25 seconds, with a stronger indication at 1.5 seconds. Again, DNB started at an elevation lower than the cladding thermocouples and propagated up the rod. This indicates a significant thermocouple effect on fuel rod response.

Cladding surface temperature measurements were made on Rod 345-1 at 0.533 m from the bottom of the fuel stack at 0° and 180° azimuthal during Tests LLR-5, -4, and -4A. The thermal response of Rod 345-1 during Tests

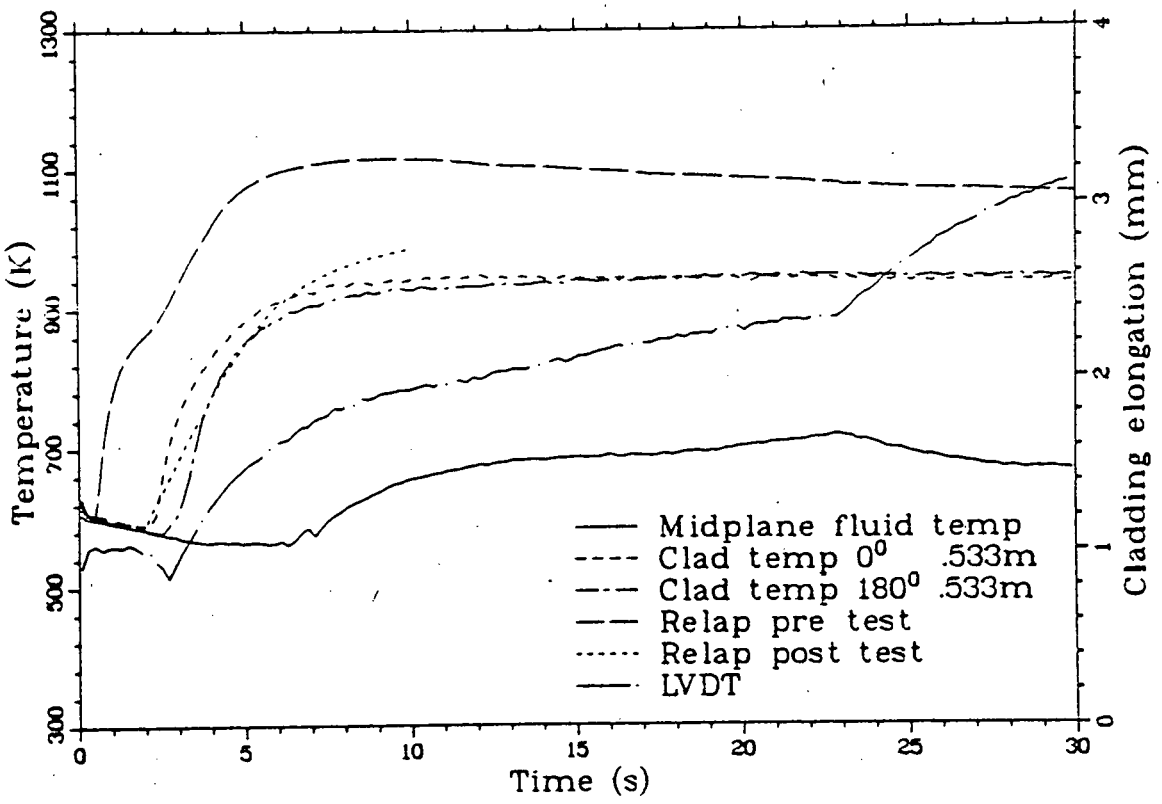

Figure 7. Thermal and mechanical behavior for Rod 312-1 for Test LLR-3.

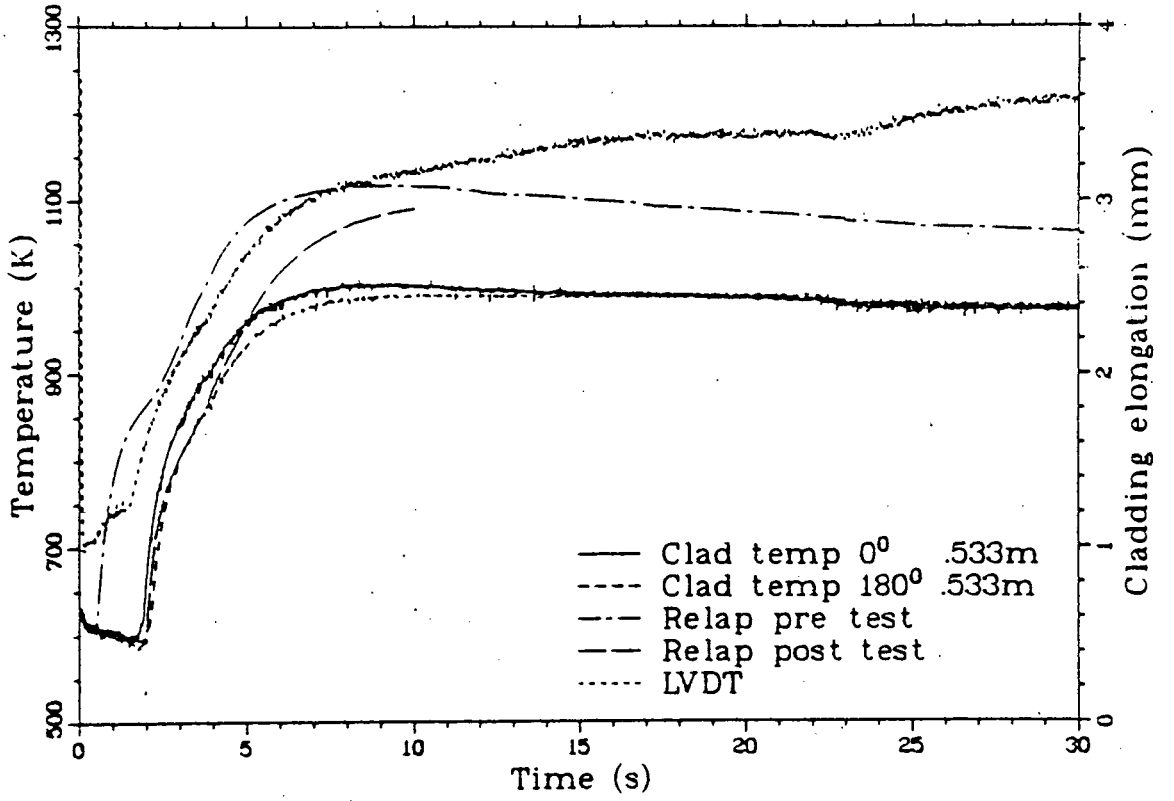

Figure 8. Thermal and mechanical behavior for Rod 312-1 for Test LLR-5.

LLR-5 and -4 was similar to the response of Rod 312-1 as indicated by the maximum temperatures shown in Table 1. Figure 10 illustrates the cladding temperature, cladding elongation, and coolant midplane temperature response of Rod 345-1 during the first 30 seconds of Test LLR-4A. The peak rod power for Rod 345-1 was 53.3 kW/m just prior to blowdown. The 180° 0.533m thermocouple overlays the 0° thermocouple throughout the blowdown transient. The cladding temperature data indicate that the rod achieved DNB at approximately 2.0 s at both thermocouple locations. Both thermocouples measured a maximum cladding temperature of 1070 K at 15 s. The cladding elongation transducer indicated a moderate increase at 0.25 s with a stronger indication at 1.5 s as CHF occurred over a significant length of the fuel rod surface below the thermocouples and then propagated up the rod. This, again, indicates a thermocouple effect on fuel rod response.

The measured fuel centerline temperature at 0.533 m for Rod 345-1 during Test LLR-4A is shown in Figure 11, with the corresponding FRAP calculated centerline temperature response. The initial centerline temperature prior to blowdown was 1920 K. The reactor was scrammed at 2.85 seconds. As shown in Figure 11, the fuel centerline temperature decreased immediately at this time as the stored energy was removed. The temperature then decreased to 1245 K at 10 s, about 150 K above the cladding surface temperature. After 10 s, the centerline temperature decreased gradually for the remainder of the blowdown transient until the rods were quenched. The measured cladding temperature at the thermocouple locations was used as the surface boundary condition to obtain the FRAP calculated fuel centerline temperature. The Ross-Stoute[3] correlation was used for the unpressurized LLR fuel rods to calculate stored energy. The FRAP calculations slightly undercalculate the stored energy for the fuel rods for the entire transient due possibly to the uncertainties that are inherent in the initial fuel rod power, fuel-to-cladding gap conductance, and UO_2 thermal conductivity.

Fuel Rod Deformation

The LLR rod cladding temperature responses and system pressure responses were evaluated to provide information on the mechanical deformation of the

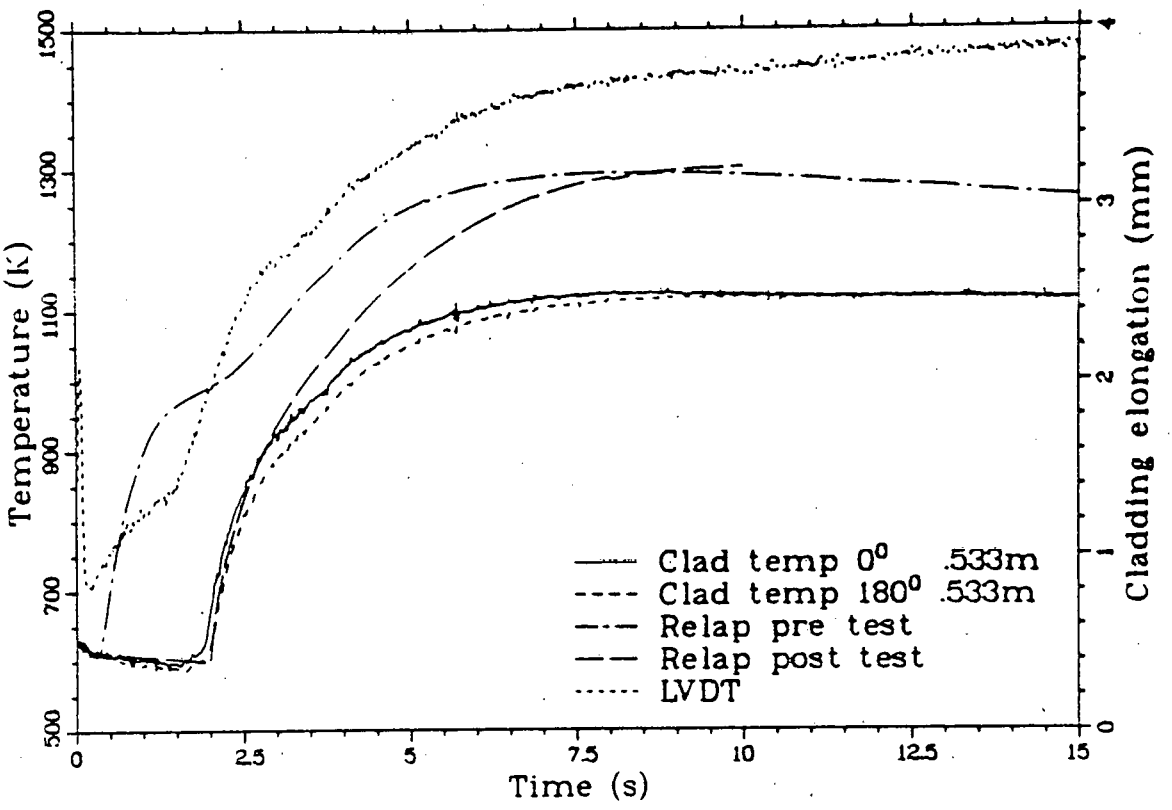

Figure 9. Thermal and mechanical behavior for Rod 312-1 for Test LLR-4.

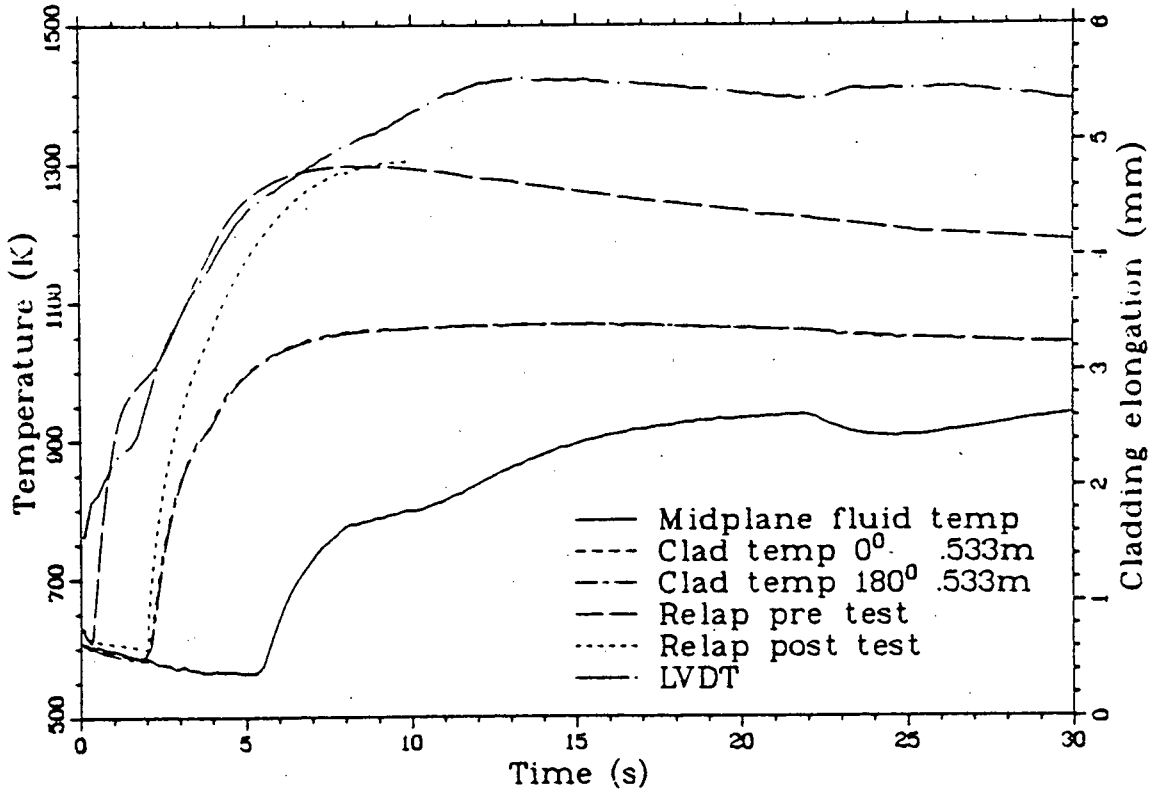

Figure 10. Thermal and mechanical behavior for Rod 345-1 for Test LLR-4A.

cladding and were compared with related data published by Olsen.[4] The results of the post-irradiation examination (visual appearance, extent of the cladding collapse, and cladding microstructural changes) also provided information to evaluate the LLR test rod damage. Finally, the fuel centerline measurements were indicative of changes from test to test in the performance of the rods during subsequent power excursions.

Fuel Rod Deformation as Evidenced by Comparison with Olsen's Criteria. Olsen has investigated zircaloy tubing deformation under isothermal, isobaric conditions. These tests were conducted on LOFT type fuel rods to determine the pressure-temperature loci for the boundaries between two-point buckling (cladding contact onto the fuel pellets at two points on the fuel circumference which results in an ovality of the cladding), uniform circumferential cladding collapse onto the fuel pellets, and waisting (plastic flow of zircaloy cladding into small pellet-to-pellet gaps in the fuel stack). The mechanical deformation that was witnessed in the LLR tests can be directly compared with the fuel rod cladding deformation criteria developed by Olsen.

Mechanical deformation of the unpressurized fuel rods occurred during the early part of the LLR blowdowns when the cladding temperatures were near their maximum values and the system pressure was still relatively high. The measured cladding temperature for Rod 312-1 during Test LLR-3 is plotted as a function of fuel rod differential pressure in Figure 12. The measured temperature-pressure history falls below the cladding buckling region, as determined by Olsen, which indicates that no permanent cladding deformation would be expected to have occurred at the thermocouple location on this rod during this test.

As shown in Figure 13, the cladding surface temperature versus differential fuel rod pressure for Rod 312-1 during Test LLR-5 indicates buckling probably occurred to this rod at the thermocouple locations. However, since DNB was achieved earlier at locations below the thermocouples, estimates of higher temperatures at lower elevations have been made. On the

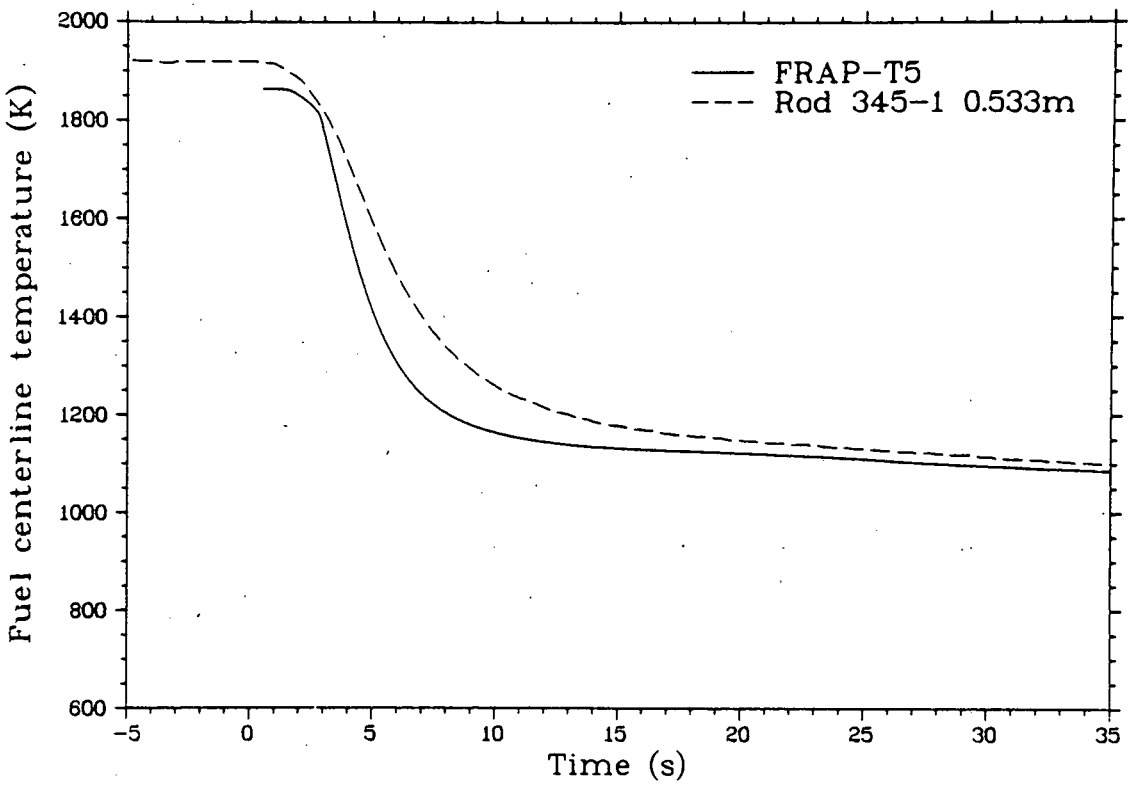

Figure 11. Comparison of fuel centerline temperature with FRAP-T5 for Rod 345-1 for Test LLR-4A.

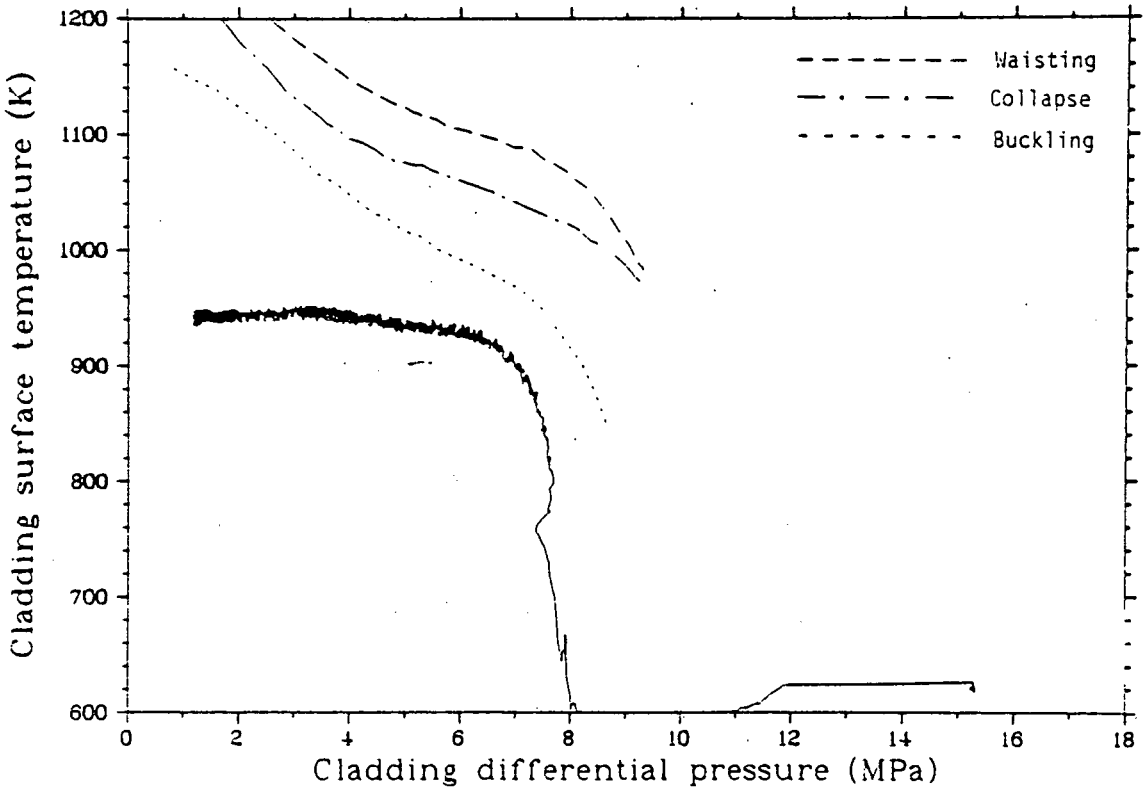

Figure 12. Surface temperature versus fuel rod differential pressure for Rod 312-1 for Test LLR-3.

basis of the response of Rod 399-2 during Test LLR-4A in which cladding temperatures of 1260 and 1205 K were measured at the 0.314 and 0.457 m locations, respectively, an estimate of 1060 K at the 0.314 m location was made for Rod 312-1. This temperature would result in local buckling and incipient uniform circumferential cladding collapse for the fuel rod.

The cladding surface temperature versus fuel rod differential pressure of Rod 312-1 during Test LLR-4 shown in Figure 14 indicates the cladding was subjected to temperatures slightly above that required to cause waisting at the thermocouple locations. Since cladding temperatures as high as 1225 K may have been achieved at the 0.314 m location, waisting probably occurred along a significant portion of the fuel rod.

The Rod 345-1 measured cladding temperature during Test LLR-4A is plotted as a function of fuel rod differential pressure in Figure 15. As shown, the cladding surface temperature versus fuel rod differential pressure indicates the cladding was subjected to temperatures slightly above that required to cause collapse at the thermocouple locations. However, cladding temperatures as high as 1155 K may have been achieved at the 0.314 m location, which would result in waisting along the greater portion of the fuel rod.

Fuel Rod Deformation as Evidenced by PIE. During the postirradiation examination, all the rods were found to be uniformly covered with a black layer of zirconium dioxide and there was no visual indication of the axial extent of film boiling. In addition, the fuel rods did not exhibit any visually discernable deformation (bowing or loss-of-diameter). However, the posttest diameter measurements indicated that the cladding of all the rods (except Rods 312-3 and 312-4 from Test LLR-3) had collapsed onto the fuel stack from about 30 to 60 cm from the bottom of the heated length.

Permanent changes to the cladding of Rod 312-1 occurred as a result of the three successive blowdowns discussed above. The cladding microstructure which corresponds to the maximum measured temperature of 1125 K at the 0.533 m location is the $\alpha + \beta$ transformation structure which exists in the temperature

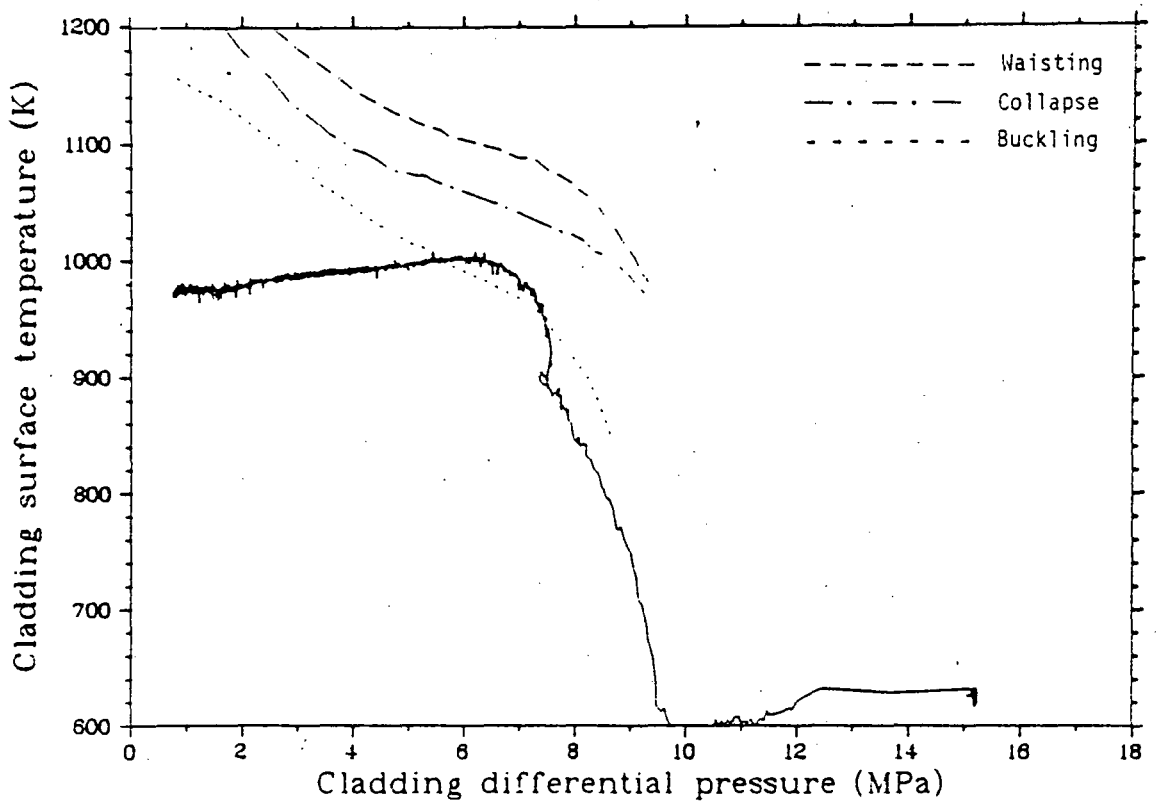

Figure 13. Surface temperature versus fuel rod differential pressure for Rod 312-1 for Test LLR-5.

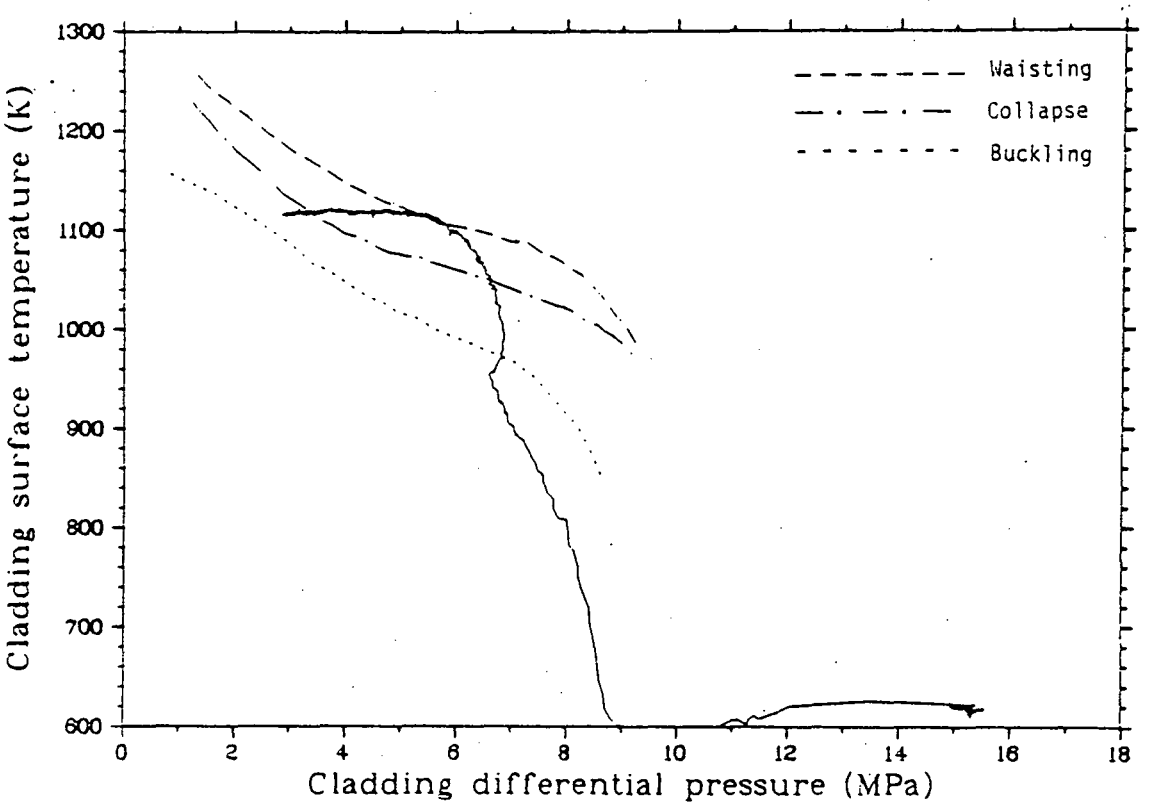

Figure 14. Surface temperature versus fuel rod differential pressure for Rod 312-1 for Test LLR-4.

range of 1100 to 1270 K. Figure 16 presents the cladding microstructure at the thermocouple junctions located 0.533 m above the bottom of the fuel stack. Equiaxed α-zircaloy structure is present throughout the entire cladding thickness, including some β precipitates at the grain boundaries, which indicates temperatures in the vicinity of 1100 to 1150 K. A longitudinal section was made at an axial elevation at 0.49 to 0.51 m above the bottom of the heated length (below the thermocouples) in the 0-180° plane to characterize the axial temperature profile of the rod. Again, a alpha plus beta zircaloy structure was observed.

Circumferential temperature gradients of 15 K were measured during Test LLR-5. The effect of these gradients on cladding microstructure was not observable. Also, the influence of the cladding thermocouples on the fuel rod response was not observable by comparing the 90-270° plane to the 0-180° plane.

The measurement of oxide layer thickness, in conjunction with applicable oxide layer growth kinetics, provides an independent estimate of cladding temperatures during testing. The oxide layer determined on the 312-1 fuel rod was evaluated to determine the extent of oxide layer growth due to steady state operation and the increased temperatures during the successive LLR transients. Rod 312-1 was at reactor operating temperatures (600 K) for approximately 241 hours. A calculation was performed to determine how much of the observed oxide thickness resulted from this exposure and a zirconium dioxide thickness of 0.7 μm was obtained. A total thickness of 3 μm was measured after the 3 transients for Rod 312-1. Zirconium dioxide and oxygen stabilized α-zirconium layers due to the steam-zircaloy reaction were measured on the external surface of the cladding, while an oxygen stabilized α-zirconium layer due to the UO_2-zircaloy reaction was measured on the inside surface of the cladding. These measurements were determined from the photomicrographs of the fuel rod. Cladding temperatures were determined based on Leistikow's out-of-pile experimental data. The maximum estimated temperature is in the range of 1140 to 1145 K which is again in good agreement with the maximum value of 1125 K measured using a cladding surface thermocouple.

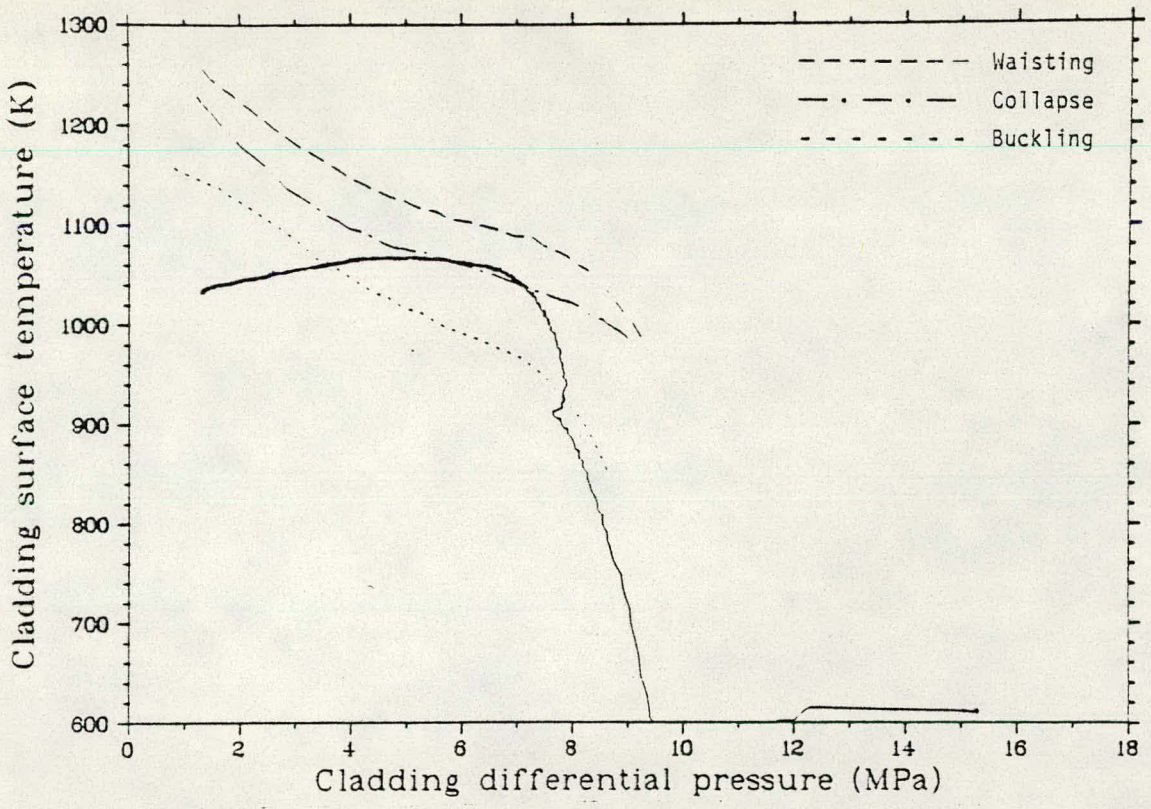

Figure 15. Surface temperature versus fuel rod differential pressure for Rod 345-1 for Test LLR-4A.

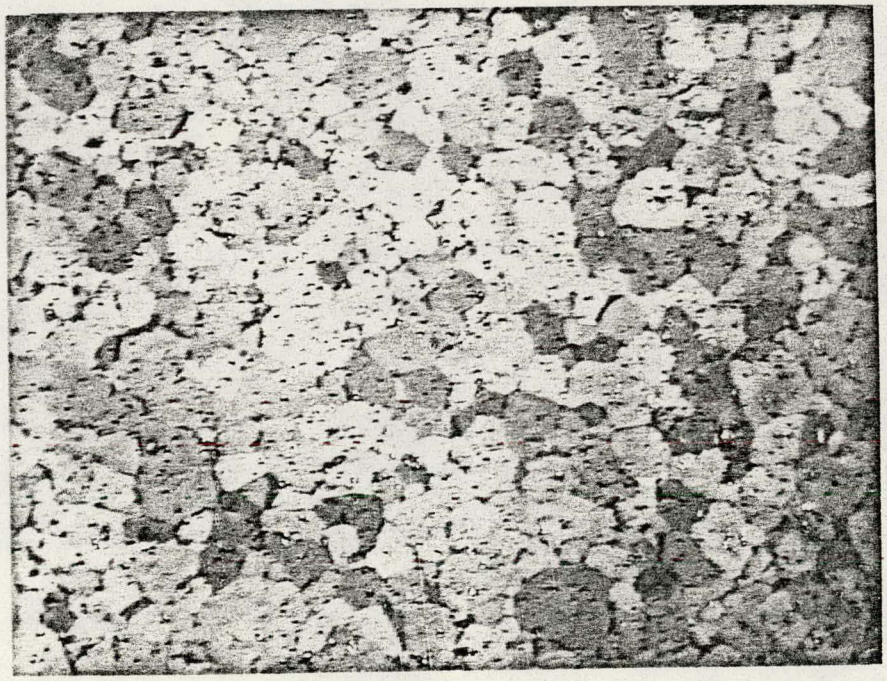

Figure 16. Rod 312-1 transverse cladding microstructure from 0.53 to 0.55 m.

Diametral measurements were made 90 degrees apart along the length of each fuel rod. The averaged data for Rod 312-1 is plotted versus the fuel stack axial length in Figure 17. The rod exhibited collapse, with the maximum diametral decrease of 0.06 mm along the rod midsection about 61 cm from the bottom of the active fuel stack. The location of maximum collapse did not correspond to the axial region of maximum power (45.7 cm). The decrease in diameter at this point was only slightly less than the maximum decrease.

Permanent changes to the cladding of Rod 345-1 also occurred as a result of the three successive blowdowns it was subjected to (LLR-5, LLR-4 and LLR-4A). A maximum temperature of 1070 K was measured at the 0.533 m location on Rod 345-1. The cladding microstructure which corresponds to this temperature is the recrystallized α-zircaloy regime which exists in the temperature range of 920 to 1100 K. Figure 18 presents the cladding transverse microstructure at the thermocouple junctions located 0.533 m above the bottom of the fuel stack. As expected, recrystallized α-zircaloy structure was present throughout the cladding thickness thereby confirming the thermocouple measurement.

A longitudinal section from 0.25 to 0.27 m above the bottom of the heated length in the 90-270° plane was made to characterize the axial temperature profile of the rod at the boundary of deformation on the fuel rod. The microstructure consisted of a high concentration of equiaxed α-zircaloy, with β precipitates at the grain boundaries. The approximate temperature range for this structure is 1150 to 1200 K. This information supports the contention that in the higher power tests the LLR test rods first departed from nucleate boiling and cladding temperatures were higher below the thermocouple locations. Minimal circumferential temperature gradients were measured on Rod 345-1 during the tests. The effect of any gradients on cladding microstructure was not observable.

The oxide layer determined on the 345-1 fuel rod was evaluated to determine the extent of oxide layer growth due to steady state operation and the increased temperatures during the successive LLR transients. Rod 345-1

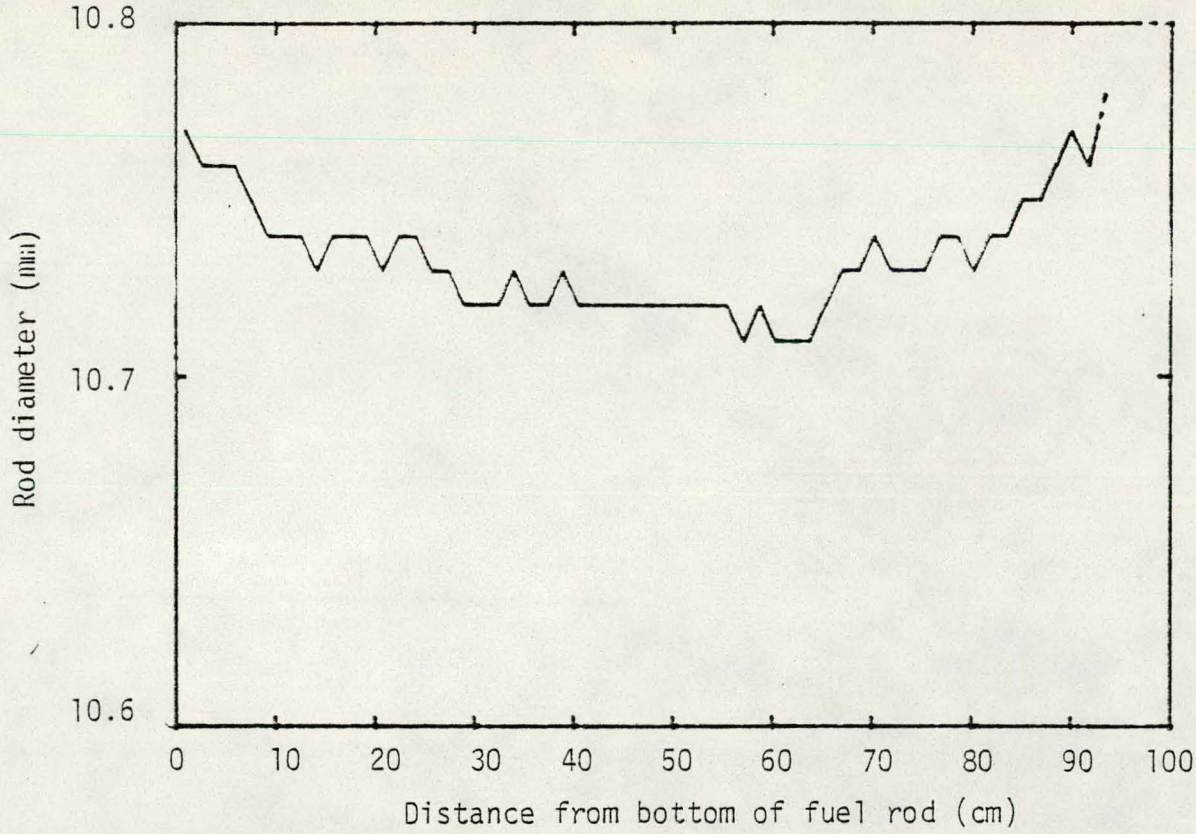

Figure 17. Postirradiation examination measurements of cladding diameter for Rod 312-1.

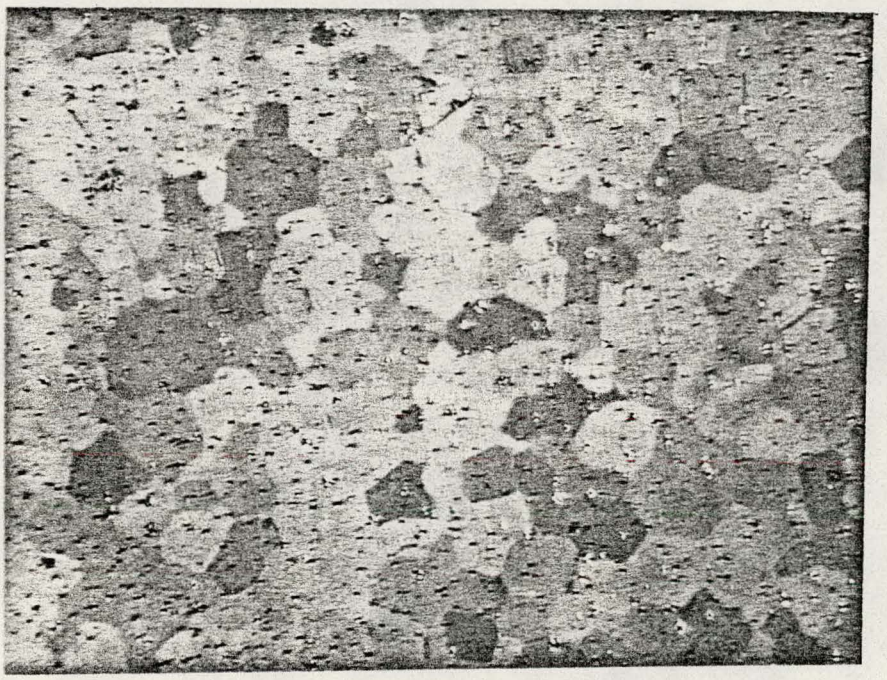

Figure 18. Rod 345-1 transverse cladding microstrucure at 0.533 m.

was at reactor operating temperatures (600 K) for approximately 89 hours. A calculation was performed to determine how much of the observed oxide thickness resulted from this exposure and a zircaloy dioxide thickness of 0.5μm was obtained. A maximum total thickness of 4μm was measured on Rod 345-1 after the 3 transients. Zirconium dioxide and oxygen stabilized α-zirconium layers due to the steam-zircaloy reaction were measured from the photomicrographs of the fuel rod on the external surface of the cladding, while an oxygen stabilized α-zirconium layer due to the UO_2-zircaloy reaction was measured on the inside surface of the cladding. Cladding temperatures were determined from these layers by using Leistikow's out-of-pile data. The maximum estimated temperature is approximately 1155 K at the 26 cm level which is above the maximum value measured using a surface thermocouple of 1070 K but consistent with the cladding microstructure as expected.

Waisting was observed along the entire axial length of Rod 345-1. Posttest diametral measurements were made 90 degrees apart along the length of each fuel rod. The averaged data for Rod 345-1 is plotted versus the fuel stack axial length in Figure 19. The rod exhibited collapse, with the maximum diametral decrease of 0.05 mm along the rod midsection from 46.5 to 65.7 cm from the bottom of the active fuel stack. The location of maximum collapse corresponded to the axial region of maximum power (45.7 m), which corresponded to the maximum pretest RELAP4 calculated cladding temperature.

It is interesting to note that the deformation witnessed on the uninstrumented fuel rod (345-2) was higher than on Rod 345-1, its companion fuel rod. During the visual examination, the rod showed severe waisting 37 to 47 cm from the bottom of the fuel stack. Posttest diametral measurements indicated that the rod exhibited collapse, with a maximum decrease in diameter of 0.06 mm along the rod midsection from 31 to 68 cm from the bottom of the heated length. This is consistent with comparison of the cladding temperatures approximated from microstructures and oxide layer thickness which indicated higher temperatures for Rod 345-2, than Rod 345-1.

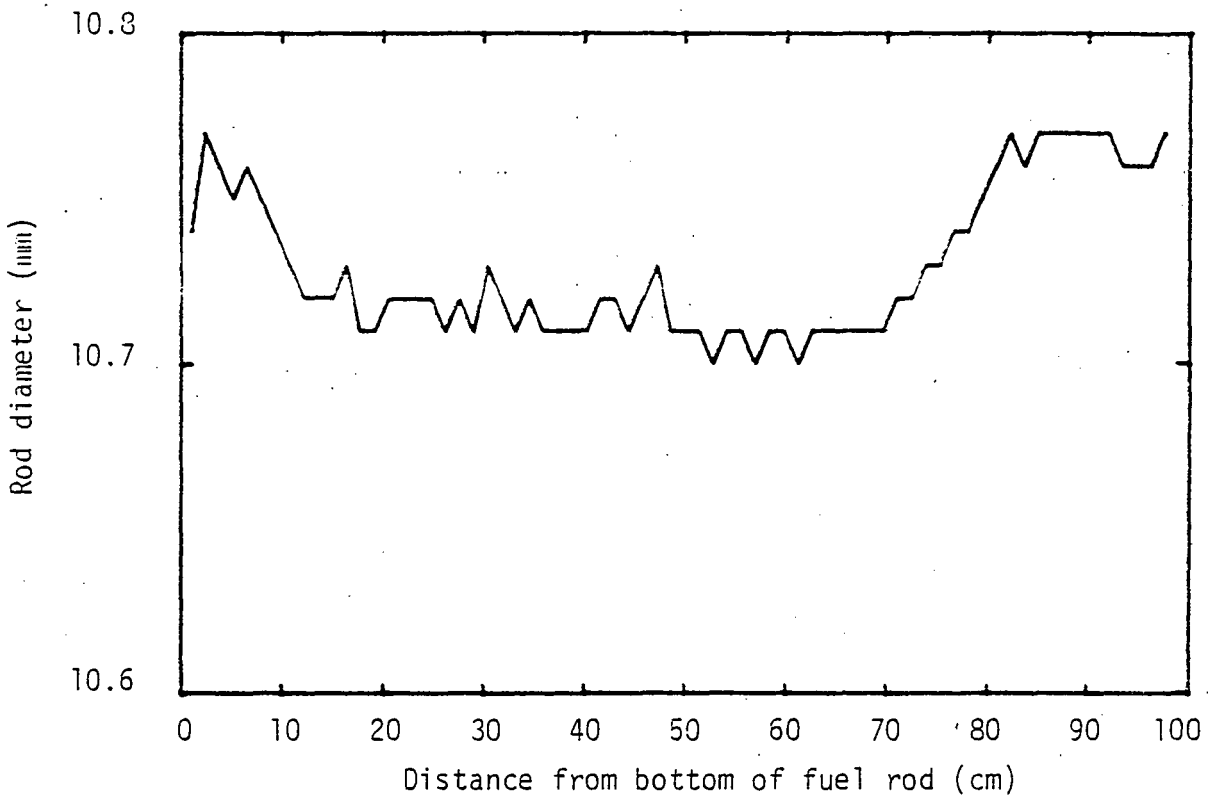

Figure 19. Postirradiation examination measurements of cladding diameter for Rod 345-1.

A plot of maximum estimated cladding temperature versus distance from the bottom of the fuel stack was constructed from the microstructure estimates from the transverse and longitudinal sections and is shown in Figure 20 for selected fuel rods. A plot of the axial temperature profile calculated by RELAP4 and normalized to 1200 K to fit through the peak measured values at the thermocouple locations is also included. The fact that higher microstructure estimates were made on the lower portion of the rods from 25 to 40 cm is again indicative of the thermocouple effects in the LLR tests. The maximum measured cladding temperatures for the rods of Tests LLR-4 and -4A are also included.

General conclusions from the PIE can be summarized as follows:

1. There is no apparent circumferential or longitudinal gradient around the thermocouples.

2. The fuel rod without thermocouples (345-2) indicated a higher cladding temperature microstructure than rods with thermocouples, suggesting a thermocouple effect.

3. Based on the posttest visual examination and diametral measurements, larger deformation was revealed on the rod without thermocouples than on the rods with thermocouples.

4. The measured cladding surface temperatures are in reasonable agreement with the temperatures estimated from the cladding microstructures.

Fuel Rod Deformation as Evidenced by Steady-State Centerline Temperatures. Steady state analyses were performed to determine whether cladding deformation could be detected by monitoring the centerline temperature. It is possible to detect fuel rod cladding collapse by observing the centerline temperature response of the fuel during steady-state operation following a LOCE. This methodology is the only positive indication of a deformed cladding condition that existed between the successive PBF/LLR

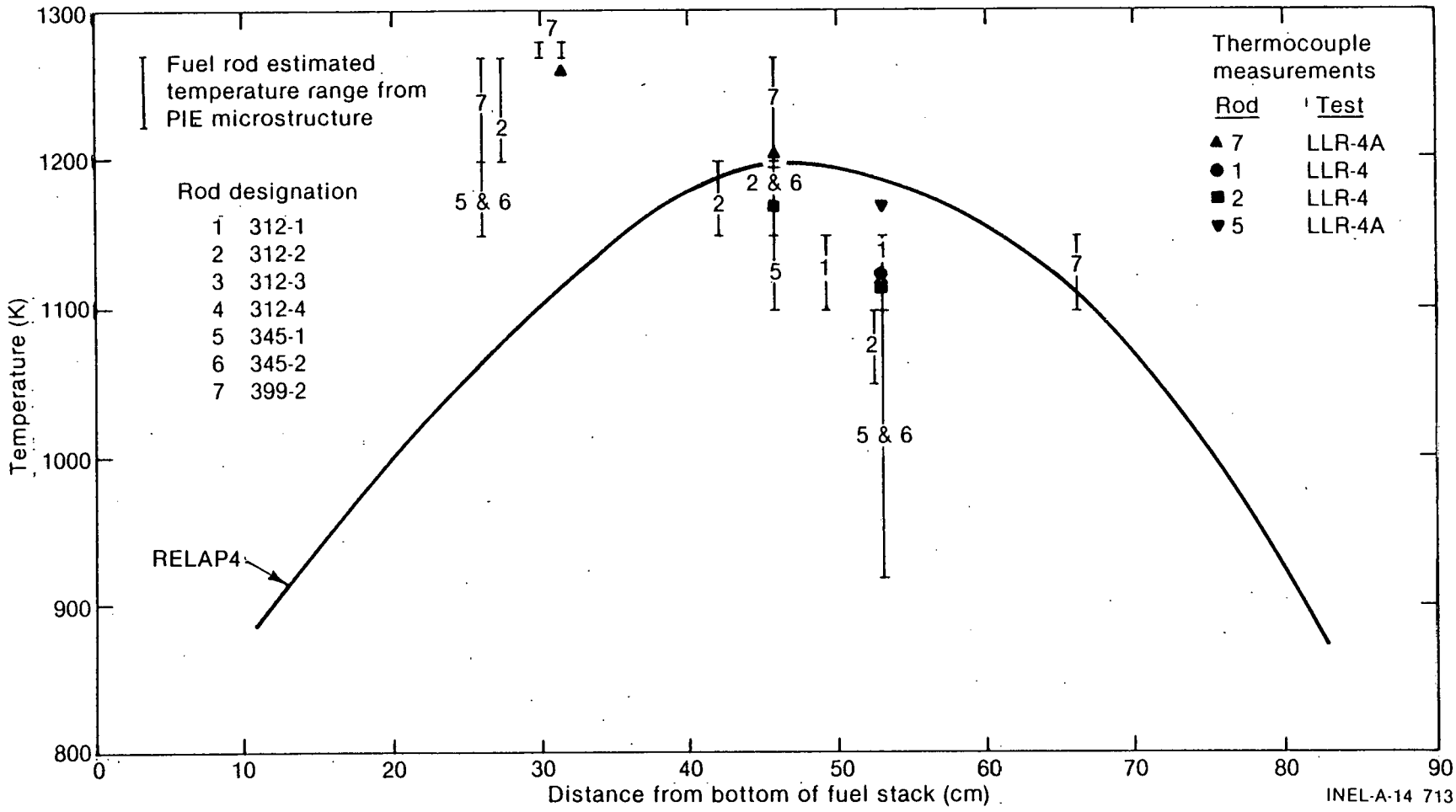

Figure 20. Comparison of maximum measured, PIE estimated (microstructure), and calculated cladding temperatures for the LLR-4 and LLR-4A tests.

transients. Therefore, the measured and FRAP predicted centerline temperature for a representative LLR test rod (Rod 345-1) for the power ramping portion of each test are presented in the following sections. The fuel rod analyses were performed in sequence paralling the LLR test sequence. Starting with each test, the fuel was ramped through preconditioning, then exposed to the LOCA blowdown, and finally, the reflood.

The centerline temperature data obtained from fuel Rod 345-1 during Tests LLR-5, -4, and -4A are illustrated in Figure 21 with the corresponding FRAP predictions. For linear heating rates less than 30 kW/m, the measured centerline temperatures for Tests LLR-5 and -4 agree closely. At heating rates greater than 30 kW/m, the data for the two tests begins to diverge. This is not attributed to cladding deformation occurring during the LLR-5 test since Olsen's criteria indicated the fuel rod only reached incipient buckling at the thermocouple locations. The difference could be attributed to significant pellet relocation during LLR-4 that resulted in an decrease in the radial thermal resistance across the fuel rod.

Comparison of the steady state centerline temperature data from Tests LLR-4 and -4A for Rod 345-1 indicates that the LLR-4A data is consistently lower than the LLR-4 data. Since waisting was verified on fuel rod 312-1 after Test LLR-4, cladding collapse probably occurred on portions of all of the other fuel rods during the LLR-4 test. The lower centerline temperature recorded during the steady state portion of the LLR-4A test is a positive indication of collapsed cladding and a higher gap conductance for Rod 345-1 prior to the LLR-4A blowdown transient.

In conclusion, based on the centerline temperature responses of Rod 345-1, it is evident that the fuel rod cladding at the thermocouple locations had not collapsed until the LLR-4 test.

CONCLUSIONS

The PBF/LLR test program consisted of four sequential LOCA experiments

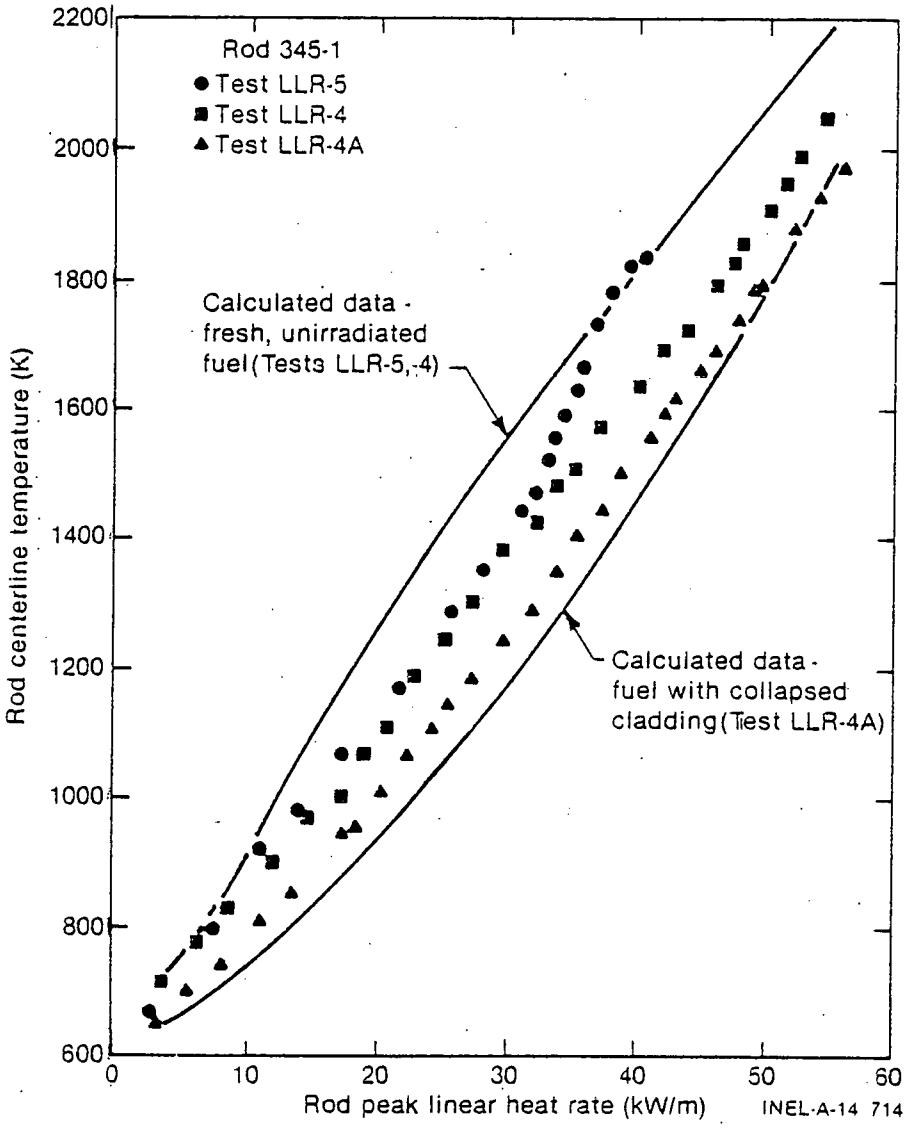

Figure 21. Comparison of steady-state response of Rod 345-1 with FRAP-T5 during Tests LLR-5, -4, and -4A.

during which seven PWR type fuel rods were evaluated. Measured cladding temperatures ranged from 870 to 1260 K when the rods were exposed to blowdown conditions similar to those expected in a PWR during a hypothesized double-ended cold leg break. The PBF/LLR Test Series fuel rods experienced the maximum mechanical deformation that would be expected to occur to the LOFT fuel rods during the LOFT L2 Power Ascension Tests. The program demonstrated that low pressure, light water reactor design fuel rods, and specifically LOFT design fuel rods, are able to withstand successive preconditioning cycles and LOCA tests without failure.

Relative to the LLR tests themselves, several conclusions can be drawn. These include: (a) the mechanical deformation of the fuel rods that was observed during the postirradiation examination was consistent with Olsen's criteria for fuel rod deformation; (b) the temperature and cladding elongation sensors indicated DNB was first observed at an elevation lower than the peak power elevation; (c) the lower elevations consequently achieved higher cladding temperatures; (d) the delay in CHF and lower cladding temperatures at the peak power elevation is attributed to thermocouple effects; (e) the RELAP4 code accurately predicted the system thermal-hydraulic behavior, but underpredicted times to CHF, and subsequently predicted higher cladding temperatures than measured at the thermocouple locations. However, the RELAP4 cladding temperature predictions may be close to the actual temperatures at locations without thermocouple attachments. During the postirradiation examination, several of the preceding conclusions were confirmed. These include: (a) thermocouple effects were obvious, resulting in lower cladding temperatures and less deformation at the thermocouple locations; and (b) RELAP4 pretest cladding temperature calculations were reasonable at elevations on the fuel rod lower than the thermocouples.

ACKNOWLEDGEMENTS

The authors express their appreciation to K. A. Dietz, R. K. McCardell, and D. R. Evans for their assistance in this study.

REFERENCES

1. D. L. Reeder, LOFT System and Test Description, NUREG/CR-0247, TREE-1208, July 1978.

2. K. R. Katsma et al., RELAP4/MOD5-A Computer Program for Transient Thermal-Hydraulic Analysis of Nuclear Reactors and Related Systems, NUREG-1335, September 1976.

3. L. J. Siefken, et al. FRAP-T5 -- A Computer Code for the Transient Analysis of Oxide Fuel Rods, NUREG/CR-0840, TREE-1281, June 1979.

4. C. S. Olsen, Zircaloy Cladding Collapse Under Off-Normal Temperature and Pressure Conditions, NUREG-1239, April 1978.

NOTICE

Work supported by the U.S. Nuclear Regulatory Commission, Office of Nuclear Regulatory Research under DOE Contract No. DE-AC07-76ID01570.